ELSEVIER

Joint linear optimization with receiver constraint for MIMO systems

Tobias P. Kurpjuhn, Michael Joham*, Josef A. Nossek

Lehrstuhl für Netzwerktheorie und Signalverarbeitung, Technische Universität München, Arcisstr. 16, 80290 München, Germany

Abstract

In this article, we propose a new linear multiple-input multiple-output (MIMO) system with the receiver matched to the transmit filter plus channel, leading to a linear transmission system which diagonalizes the MIMO channel into its eigenspace similar to joint transmit and receive filter optimization (joint TX/RX optimization). The proposed transmission scheme is shown to achieve comparable bit-error performance to joint TX/RX optimization in the case of adaptive modulation. Furthermore, the proposed scheme outperforms joint TX/RX optimization in terms of complexity: if neither the possibility of feedback, nor sufficient computational resources at both sides of the link are available, the joint TX/RX optimization approach is not applicable contrary to the proposed approach. We investigate different optimization criteria well known from linear precoder design and joint TX/RX optimization: maximizing the signal-to-noise ratio, removing the interference, and minimizing the mean square error. Closed-form solutions are derived for these cases.
© 2005 Elsevier GmbH. All rights reserved.

Keywords: MIMO; Linear filtering; Joint optimization; Adaptive modulation

1. Introduction

Contrary to the approaches of receive-only [1] and transmit-only optimization [2,3], where only one side of the communication link is optimized with respect to a specific optimization criterion while the other side of the communication link is assumed fixed and a priori known, it is also possible to assume a cooperative design of the signal processing at the transmitter and the receiver. This optimization approach is denoted as *joint* transmit and receiver filter (*TX/RX*) *optimization*. Joint TX/RX optimization is a well researched and understood approach to deal with multiple-input multiple-output (MIMO) systems (e.g. [4–10]) where the receive and transmit filters result from one optimization, as described in Section 4.

A big disadvantage of the joint TX/RX optimization is the required computational complexity at both sides of the communication link or alternatively, a large amount of feedback. Since the design of the linear precoder as well as the linear receiver evolve from one joint optimization approach, either both sides of the communication link have to perform the optimization, or the result of the optimization is computed at one side of the communication link for the price of having to transmit the optimization result to the other side of the communication link. If *neither* the possibility of feedback, *nor* sufficient computational resources at both sides of the link are available, the joint TX/RX optimization approach is not applicable.

To overcome this dilemma we propose the new *semi-joint TX/RX optimization* approach, where one side of the communication link is simplified with respect to the computational complexity, i.e. a restricted receiver structure. In this article, we will derive a MIMO system where we assume a simplified receiver structure such, that the receiver is a

matched-filter, however, not only to the channel but also to the precoding filter.[1] This assumption is advantageous in two ways.

First, we end up with a decomposition of the channel into its eigenmodes similar to joint TX/RX optimization. This diagonalization of the channel provides good conditions for spatial multiplexing: due to the diagonalization of the MIMO channel there is no *inter-stream interference* between parallel transmitted data streams.

Second, the pilot symbols necessary for channel estimation at the receiver can be transmitted time multiplexed with the data and do not have to bypass the precoding filter. Therefore, the receiver estimates the combination of the precoding filter and the channel together with the imperfections of the transmission chain (e.g. erroneous synchronization or calibration).

Our contributions are as follows:

- We obtain *closed-form solutions* for three semi-joint TX/RX optimizations.
- We highlight that the TX-only (likewise, the RX-only) approaches clearly outperform the joint and semi-joint TX/RX optimizations in terms of BER for systems with fixed modulation alphabet.
- We perform a thorough comparison of the joint and semi-joint TX/RX optimizations with adaptive modulation for the cases of instantaneous and long-term channel knowledge.

2. Overview and notation

The article is organized as follows: the system model of the considered linear MIMO transmission chain is explained in Section 3. Section 4 reviews the derivation and solution of the joint TX/RX optimizations. The approach of *semi-joint TX/RX optimization* is described in Section 5. Both approaches, joint TX/RX optimization and semi-joint optimization, are compared in Section 6 where also an extension towards adaptive modulation and exploitation of long-term properties of the channel is performed. A conclusion is drawn in Section 7.

The following notation is used: vectors and matrices appear as bold lower-case and bold capital letters, respectively. With this notation $\mathbf{1}$ denotes the identity matrix. Commonly used operators are: $E\{\cdot\}$ denotes the expectation operator, tr(.) sums up the diagonal elements of its argument, $\|.\|_2$ is the Euclidean norm, $(\cdot)^*$ denotes complex conjugate, $(\cdot)^{\mathrm{T}}$ denotes transposed and $(\cdot)^{\mathrm{H}}$ conjugate transposed, $\otimes$ is the Kronecker product, and vec$(\cdot)$ performs a vectorization of the argument by stacking the columns.

---

[1] Note, that other receiver concepts, like the zero-forcing or Wiener filter approach, also diagonalize the MIMO channel. However, since the MF already is sufficient to diagonalize the channel we choose it due to its simplicity with respect to the computational complexity.
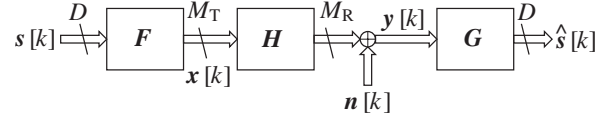

Fig. 1. Block diagram for linear TX and RX processing.

3. MIMO system model

The data $s[k] \in \mathbb{C}^D$ are filtered by the precoder $\boldsymbol{F} \in \mathbb{C}^{M_{\mathrm{T}} \times D}$ at the *base station* (BS) to form the transmit signal. In the following, we assume that all transmit filters use the whole available transmit power P_t, i.e.

$$E\left\{\|\boldsymbol{F}s[k]\|_2^2\right\} = P_t.$$

After propagation over the frequency flat single-user MIMO channel $\boldsymbol{H} \in \mathbb{C}^{M_{\mathrm{R}} \times M_{\mathrm{T}}}$ with M_{T} transmit and M_{R} receive antenna elements and perturbation by the Gaussian noise $\boldsymbol{n}[k]$, the received signal is passed through the linear receive filter $\boldsymbol{G} \in \mathbb{C}^{D \times M_{\mathrm{R}}}$ leading to the estimate (cf. Fig. 1)

$$\hat{s}[k] = \boldsymbol{GHF}s[k] + \boldsymbol{Gn}[k] \in \mathbb{C}^D. \tag{1}$$

The noise is complex Gaussian distributed with zero mean and spatial covariance matrix $\boldsymbol{R}_n$ which computes as

$$\boldsymbol{R}_n = E\left\{\boldsymbol{n}[k]\boldsymbol{n}^{\mathrm{H}}[k]\right\} \in \mathbb{C}^{M_{\mathrm{R}} \times M_{\mathrm{R}}}.$$

The corresponding spatial covariance matrix of the signal is denoted as $\boldsymbol{R}_s \in \mathbb{C}^{D \times D}$. In the following we will restrict the signal covariance matrix to $\boldsymbol{R}_s = \sigma_s^2 \mathbf{1}$. The derivation for general $\boldsymbol{R}_s$ can be found in [11]. Furthermore, we restrict ourselves to transmitting a constant data rate of b bits per channel use over D independent data streams with average transmit power P_t. Furthermore, we restrict to MIMO systems with $D = \min(M_{\mathrm{T}}, M_{\mathrm{R}})$. For the general case, see [11].

All linear precoders and receivers in the remainder of this paper can be expressed as a function of the eigensystem of the following matrix product:

$$\boldsymbol{R}_H = \boldsymbol{H}^{\mathrm{H}}\boldsymbol{R}_n^{-1}\boldsymbol{H} = [V \ \tilde{V}]\begin{pmatrix} \boldsymbol{\Lambda} & \mathbf{0} \\ \mathbf{0} & \tilde{\boldsymbol{\Lambda}} \end{pmatrix}[V \ \tilde{V}]^{\mathrm{H}}, \tag{2}$$

where the matrices $\boldsymbol{\Lambda}$ and V contain the dominant (non-zero) eigenvalues and the corresponding eigenvectors. We assume that the eigenbase in V and $\boldsymbol{\Lambda}$ is sorted such, that in $\boldsymbol{\Lambda} = \mathrm{diag}\{\lambda_1, \lambda_2, \ldots, \lambda_D\}$ we have $\lambda_1 \geqslant \lambda_2 \geqslant \cdots \geqslant \lambda_D$. Furthermore, the ith column of the eigenbase V is the unit norm vector $\boldsymbol{v}_i$.

4. Joint linear TX/RX optimization

The idea of joint TX/RX optimization is to perform a cooperative design of the linear precoder and the linear receiver. It is intuitively clear that this approach will obtain

the best performance of the linear signal processing methods with respect to the chosen optimization criterion.

4.1. Joint matched filter

Maximizing the signal-to-noise ratio (SNR) at the receiver via a joint optimization of the linear transmitter $\boldsymbol{F}$ and the linear receiver $\boldsymbol{G}$ leads to the joint MF design

$$\left\{ \boldsymbol{F}_{\text{MF}}^{\text{jt}}, \boldsymbol{G}_{\text{MF}}^{\text{jt}} \right\} = \underset{\{\boldsymbol{F},\boldsymbol{G}\}}{\operatorname{argmax}} \frac{|E\left\{ \hat{\boldsymbol{s}}^{\text{H}}[k]\boldsymbol{s}[k] \right\}|^2}{E\left\{ \boldsymbol{s}^{\text{H}}[k]\boldsymbol{s}[k] \right\} E\left\{ \|\boldsymbol{G}\boldsymbol{n}[k]\|_2^2 \right\}}$$

s.t. $\quad E\left\{ \|\boldsymbol{x}[k]\|_2^2 \right\} = P_t.$

As already shown in [10,12–15], the solution to above optimization reads as

$$\boldsymbol{F}_{\text{MF}}^{\text{jt}} = \sqrt{\frac{P_t}{\sigma_s^2}} \boldsymbol{v}_1 \frac{\boldsymbol{c}^{\text{T}}}{\|\boldsymbol{c}_2\|}$$

and

$$\boldsymbol{G}_{\text{MF}}^{\text{jt}} = \alpha \frac{\boldsymbol{c}^*}{\|\boldsymbol{c}_2\|} \boldsymbol{v}_1^{\text{H}} \boldsymbol{H}^{\text{H}} \boldsymbol{R}_n^{-1}, \tag{3}$$

where the scalar $\alpha \in \mathbb{C}$ is arbitrary, since it does not influence the SNR γ, and $\boldsymbol{c} \in \mathbb{C}^D$ is an arbitrary vector of unit norm. When choosing α to be a scalar Wiener filter to recover the signal amplitude, we get

$$\alpha = \frac{\sqrt{P_t}}{P_t \lambda_1 + \sqrt{\sigma_s^2}} \in \mathbb{R}_+.$$

Note that all transmit power P_t is transmitted over the eigenvector $\boldsymbol{v}_1$ corresponding to the maximum eigenvalue λ_1 of $\boldsymbol{R}_H$. Thus, the joint MF always provides a rank 1 transmission situation.

4.2. Joint zero-forcing filter

The cooperative design of the linear precoder and the linear receiver eliminating the inter-stream-interference and establishing the same unit path attenuation on every substream, i.e. $\boldsymbol{GHF} = \boldsymbol{1}$, leads to the joint ZF solution. However, different approaches are possible.

In [10], the joint ZF is derived by eliminating the inter-stream-interference and demanding an identical SNR on each data stream which achieves the same BER on each data stream for fixed modulation schemes. Consequently, this approach is denoted as *equal-error design*. The joint ZF filter with *equal error design* can be written as [10]

$$\boldsymbol{F}_{\text{ZF}}^{\text{equal}} = \sqrt{\frac{P_t}{\sigma_s^2 \operatorname{tr}(\boldsymbol{\Lambda}^{-1})}} \boldsymbol{V} \boldsymbol{\Lambda}^{-1/2}$$

and

$$\boldsymbol{G}_{\text{ZF}}^{\text{equal}} = \sqrt{\frac{\sigma_s^2 \operatorname{tr}(\boldsymbol{\Lambda}^{-1})}{P_t}} \boldsymbol{\Lambda}^{-1/2} \boldsymbol{V}^{\text{H}} \boldsymbol{H}^{\text{H}} \boldsymbol{R}_n^{-1}. \tag{4}$$

The achieved SNR on each data stream computes as

$$\gamma = \frac{P_t}{\sigma_s^2 \operatorname{tr}(\boldsymbol{\Lambda}^{-1})}.$$

Note, that contrary to the previous solution of the joint MF the joint ZF does not switch off any data stream.

As an alternative approach to derive the joint ZF filter it is also possible to minimize the MSE between the data symbols $\boldsymbol{s}[k]$ and their estimates $\hat{\boldsymbol{s}}[k]$ under the transmit power constraint

$$\left\{ \boldsymbol{F}_{\text{ZF}}^{\text{jt}}, \boldsymbol{G}_{\text{ZF}}^{\text{jt}} \right\} = \underset{\{\boldsymbol{F},\boldsymbol{G}\}}{\operatorname{argmin}} \, E\left\{ \|\boldsymbol{s}[k] - \hat{\boldsymbol{s}}[k]\|_2^2 \right\}$$

s.t. $\quad \hat{\boldsymbol{s}}[k]|_{\boldsymbol{n}[k]=0} = \boldsymbol{s}[k] \quad \text{and} \quad E\left\{ \|\boldsymbol{x}[k]\|_2^2 \right\} = P_t. \tag{5}$

With the Lagrangian multiplier method, we find for the solution of the joint ZF approach minimizing the MSE

$$\boldsymbol{F}_{\text{ZF}}^{\text{jt}} = \sqrt{\frac{P_t}{\sigma_s^2 \operatorname{tr}(\boldsymbol{\Lambda}^{-1})}} \boldsymbol{V} \boldsymbol{\Lambda}^{-1/4}$$

and

$$\boldsymbol{G}_{\text{ZF}}^{\text{jt}} = \sqrt{\frac{\sigma_s^2 \operatorname{tr}(\boldsymbol{\Lambda}^{-1})}{P_t}} \boldsymbol{\Lambda}^{-3/4} \boldsymbol{V}^{\text{H}} \boldsymbol{H}^{\text{H}} \boldsymbol{R}_n^{-1}. \tag{6}$$

Again, this joint ZF does not switch off any data stream.

4.3. Joint Wiener filter

The minimization of the MSE between the transmitted symbols $\boldsymbol{s}[k]$ and the estimates $\hat{\boldsymbol{s}}[k]$ by a cooperative design of the linear precoder $\boldsymbol{F}$ and the linear receiver $\boldsymbol{G}$ with transmit power constraint leads to the joint WF optimization

$$\left\{ \boldsymbol{F}_{\text{WF}}^{\text{jt}} \boldsymbol{G}_{\text{WF}}^{\text{jt}} \right\} = \underset{\{\boldsymbol{F},\boldsymbol{G}\}}{\operatorname{argmin}} \, E\left\{ \|\boldsymbol{s}[k] - \hat{\boldsymbol{s}}[k]\|_2^2 \right\}$$

s.t. $\quad E\left\{ \|\boldsymbol{x}[k]\|_2^2 \right\} = P_t. \tag{7}$

The joint WF solution is [7,8,10,16]

$$\boldsymbol{F}_{\text{WF}}^{\text{jt}} = \frac{1}{\sigma_s} \boldsymbol{V} \sqrt{(\mu^{-1/2} \sigma_s^2 \boldsymbol{\Lambda}^{-1/2} - \boldsymbol{\Lambda}^{-1})_+}$$

and

$$\boldsymbol{G}_{\text{WF}}^{\text{jt}} = \sqrt{(\mu^{1/2} \sigma_s^2 \boldsymbol{\Lambda}^{1/2} - \mu\boldsymbol{1})_+} \boldsymbol{\Lambda}^{-1} \boldsymbol{V}^{\text{H}} \boldsymbol{H}^{\text{H}} \boldsymbol{R}_n^{-1}, \tag{8}$$

where the Lagrangian multiplier $\mu \in \mathbb{R}$ has to be chosen to fulfill the transmit power constraint. The $(\cdot)_+$ operator sets all negative elements to zero.

Note, that the joint WF converges to the joint MF solution for very low SNR, while it converges to the joint ZF solution that minimizes the MSE (see Eq. (6)) for high SNR. Since the joint MF transmits only one data stream over the dominant eigenmode of the channel and the joint ZF always uses all eigenmodes of the channel for data transmission,

the joint WF approach successively increases the number of used eigenmodes with increasing SNR. This behavior can also be recognized in the solution of $F_{\mathrm{WF}}^{\mathrm{jt}}$ and $G_{\mathrm{WF}}^{\mathrm{jt}}$ where the operator $(\cdot)_+$ switches off the data streams, whose corresponding matrix entries are less than zero. The power allocation is accomplished such, that the weakest eigenmodes of the channel are not used, while in the remaining eigenmodes more power is allocated in the weaker eigenmodes to minimize the MSE.

5. Transmit optimization with fixed receiver strategy

The joint TX/RX optimization described in Section 4 provides a cooperative design of the linear precoder F and the linear receiver G to perform the previously described conventional optimization criteria:

- maximizing the SNR after the receiver,
- eliminating the inter-stream-interference, and
- minimizing the MSE between $s[k]$ and $\hat{s}[k]$.

The joint TX/RX optimization represents the optimum approach that can be achieved with linear transmit/receive processing in terms of the mentioned optimization criteria. If there is not enough feedback available and additionally both sides of the communication link do not offer the required computational power to perform the optimization task, a different approach has to be taken to design the transmit and receive processing. To this end an approach of *semi-joint TX/RX optimization* is described which has two major advantages: First, it does not require a large amount of computational complexity at the receiver side. Second, no feedback is necessary, if the channel state information is available at the transmitter. This makes the new approach especially attractive in time division duplex systems, where the channels of the two links are reciprocal and the transmitter can estimate the channel during reception in the other link.

In this system setup with restricted receiver structure the linear precoder as well as the linear receiver are jointly optimized, however, the receiver is limited to a MF to the channel plus precoder and a scaling $g \in \mathbb{R}$ to recover the signal amplitude. We will denote the proposed MIMO processing scheme *semi-joint optimization* [15]. The block diagram of this new system setup is illustrated in Fig. 2.
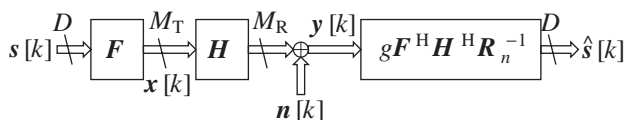

Fig. 2. Block diagram for linear TX and RX processing with restricted receiver structure.

The transmission equation of above system is given as

$$\hat{s}[k] = gF^{\mathrm{H}}H^{\mathrm{H}}R_n^{-1}(HFs[k] + n[k]). \tag{9}$$

In the sequel, we will optimize the components of the system in Fig. 2 by maximizing the SNR after the receiver (SemiMF), eliminating the interference (SemiZF), and minimizing the MSE (SemiWF).

5.1. Semi-joint matched filter

The semi-joint MF is found by maximizing the SNR after the receiver $gF^{\mathrm{H}}H^{\mathrm{H}}R_n^{-1}$ with transmit power constraint

$$\{F_{\mathrm{MF}}, g_{\mathrm{MF}}\} = \underset{\{F,g\}}{\arg\max}\ \gamma \quad \text{s.t.} \quad E\left\{\|x[k]\|_2^2\right\} = P_t, \tag{10}$$

where the SNR can be expressed as

$$\gamma = \frac{|E\left\{\hat{s}^{\mathrm{H}}[k]s[k]\right\}|^2}{E\left\{s^{\mathrm{H}}[k]s[k]\right\}E\left\{\|gF^{\mathrm{H}}H^{\mathrm{H}}R_n^{-1}n[k]\|_2^2\right\}}.$$

We obtain as solution (see Appendix A.1)

$$F_{\mathrm{MF}}^{\mathrm{semi}} = \sqrt{\frac{P_t}{\sigma_s^2}}v_1 c^{\mathrm{T}}$$

and

$$g_{\mathrm{MF}}^{\mathrm{semi}} = \frac{1}{P_t\lambda_1 + 1}, \tag{11}$$

where $c \in \mathbb{C}^D$ is an arbitrary vector of unit norm. With this setup the joint MF and the semi-joint MF are identical. Note, that the semi-joint MF also transmits only one data stream as in the case of the joint MF.

5.2. Semi-joint zero-forcing filter

Designing a linear precoder under the restriction of a linear MF receiver to eliminate the inter-stream interference where we simultaneously minimize the MSE leads to the semi-joint ZF approach. The optimization with transmit power constraint can be written as (cf. Eq. (5))

$$\left\{F_{\mathrm{ZF}}^{\mathrm{semi}}, g_{\mathrm{ZF}}^{\mathrm{semi}}\right\} = \underset{\{F,g\}}{\arg\min}\ E\left\{\|\hat{s}[k] - s[k]\|_2^2\right\}$$

$$\text{s.t.} \quad E\left\{\|x[k]\|_2^2\right\} = P_t \quad \text{and} \quad \hat{s}[k]|_{n[k]=0} = s[k]. \tag{12}$$

The solution according to Appendix A.2 can be written as

$$F_{\mathrm{ZF}}^{\mathrm{semi}} = \sqrt{\frac{P_t}{\sigma_s^2\,\mathrm{tr}(\Lambda^{-1})}}V\Lambda^{-1/2}$$

and

$$g_{\mathrm{ZF}}^{\mathrm{semi}} = \frac{\sigma_s^2\,\mathrm{tr}(\Lambda^{-1})}{P_t}. \tag{13}$$

The solution of the semi-joint ZF approach achieves a perfect inter-stream interference elimination and the whole transmission chain between the symbols $s[k]$ and $\hat{s}[k]$ is reduced to the identity matrix. Like the joint ZF approach, the semi-joint ZF approach does not switch off eigenmodes of the channel.

Moreover, the semi-joint ZF is identical to the joint ZF providing equal SNR on each data stream, cf. Eq. (4).

5.3. Semi-joint Wiener filter

Minimizing the MSE between the receive filter output $\hat{s}[k]$ and the signal $s[k]$ with the special choice of a linear MF receiver produces the semi-joint WF solution. The optimization under the transmit power constraint can be expressed as

$$\left\{ F_{WF}^{semi}, g_{WF}^{semi} \right\} = \underset{\{F,g\}}{\operatorname{argmin}} \; E\left\{ \| \hat{s}[k] - s[k] \|_2^2 \right\}$$

s.t. $\quad E\left\{ \| x[k] \|_2^2 \right\} = P_t.$

Expanding the cost-function of the optimization yields (cf. Eq. (9))

$$\left\{ F_{WF}^{semi}, g_{WF}^{semi} \right\} = \underset{\{F,g\}}{\operatorname{argmin}} \; \operatorname{tr}\Big[g^2 F^H R_H F \\ \times (g F^H R_H F - 1)^2 \sigma_s^2 \Big]$$

s.t. $\quad \sigma_s^2 \operatorname{tr}(FF^H) = P_t. \qquad (14)$

The solution can be written according to A.3 as

$$F_{WF}^{semi} = \sqrt{\frac{\operatorname{tr}(\Psi)}{2\sigma_s^2 \operatorname{tr}(\Psi - \Psi^2)}} V \Lambda^{-1/2} \Psi^{1/2}$$

and

$$g_{WF}^{semi} = 2\sigma_s^2 \frac{\operatorname{tr}(\Psi - \Psi^2)}{\operatorname{tr}(2\Psi - \Psi^2)} \qquad (15)$$

with $\Psi = (1 + \mu'' \Lambda^{-1})_+$. The solution for the semi-joint optimization can be found in an iterative procedure, where the parameter μ'' is chosen such to fulfill the transmit power constraint.

Note, that the semi-joint WF converges to the semi-joint MF for low SNR and to the semi-joint ZF for high SNR. Also note, that the semi-joint WF solution has the same property of the joint WF to successively increase the number of used data streams with increasing SNR.

6. Simulation and comparison

In this section, we present the simulation results of the joint TX/RX optimization and the semi-joint optimization where we will also take into account the performance of the transmit-only approaches as reference for the optimization

only on one side of the communication link, e.g. the transmitter. All results are the mean of 50 000 randomly chosen channel realizations obtained by Monte-Carlo simulations.

6.1. Fixed QPSK modulation

The core assumption for the following simulations is a fixed modulation format of QPSK, a flat Rayleigh fading channel $H \in \mathbb{C}^{4 \times 4}$, i.e. $M_T = 4$ transmit and $M_R = 4$ receive antenna elements, where each entry is i.i.d. complex Gaussian distributed with zero mean and unit variance, a fixed transmission rate of 8 bits per channel use, and complex Gaussian distributed noise $n[k]$ with zero mean and covariance $R_n = \sigma_n^2 \mathbf{1}$. To ensure the required data rate, always 4 data streams are transmitted. The performance measures are MSE and uncoded BER.

In addition to the receiver structures (see Figs. 1 and 2), we have added a scalar WF at the receiver to allow a fair comparison with respect to the MSE: especially in the case of transmit-only processing, a correct amplitude cannot be guaranteed at the receiver without a scalar WF.

Figs. 3 and 4 show the MSE and uncoded BER as function of the transmit SNR, respectively, for the three linear transmission strategies: the joint TX/RX optimization, the semi-joint optimization, and the transmit-only optimization. If we look at the MSE results of the different joint TX/RX optimization approaches in Fig. 3 we can see that the joint WF achieves the best performance with respect to the MSE compared to all other approaches, as it was demanded by the optimization in Eq. (7). Moreover, it converges to the joint MF for low SNR, while it converges with the joint ZF approach minimizing the MSE. We also see, that the performance of the semi-joint WF coincides with the joint WF at low SNR, but loses performance with increasing SNR. The TX-only WF starts with a worse performance compared
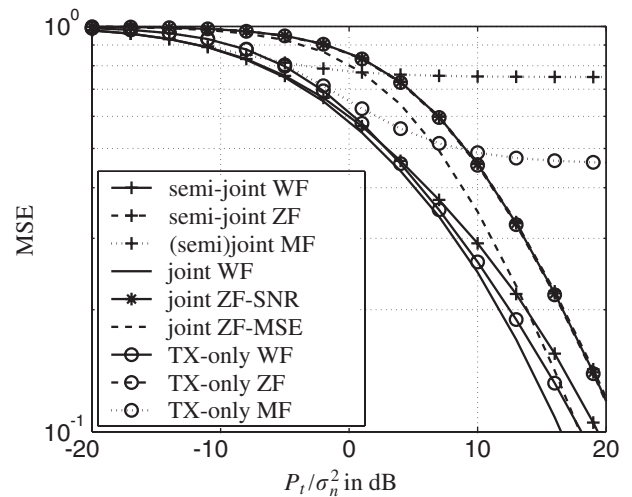

Fig. 3. MSE of the three transmission strategies as function of the transmit SNR for fixed QPSK modulation.
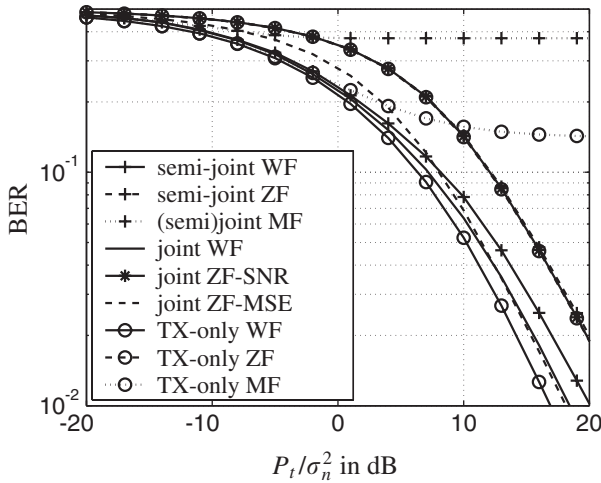
Fig. 4. BER of the three transmission strategies as function of the transmit SNR for fixed QPSK modulation.

to the joint and semi-joint WF approaches but outperforms the semi-joint WF at SNR values above approximately 3 dB. However, it is not achieving the performance of the joint WF.

Among the ZF strategies the joint ZF approach minimizing the MSE achieves best performance compared to the joint ZF demanding equal SNR, semi-joint ZF and TX-only ZF approach. The semi-joint ZF and the TX-only ZF approach achieve a perfect inversion of the channel, however, with the restricted/simplified receiver structure it is not possible to minimize the MSE of each data stream. The receiver structure of the joint ZF approach however, can be designed to achieve a minimization of the MSE of each data stream. Note, that the MSE of the TX-only ZF, the semi-joint ZF, and the joint ZF-SNR approach are identical in this case where $R_s = \sigma_s^2 \mathbf{1}$ and $R_n = \sigma_n^2 \mathbf{1}$. This is due to the fact, that

- in the TX-only ZF approach, a perfect inversion of the channel is accomplished. With the very simple receiver consisting only of a scalar WF, the MSE is only determined by a scaled version of the noise covariance matrix R_n. The MSE is identical for each data stream;
- in the semi-joint ZF case, also a perfect inversion of the channel is accomplished. The special choice of the linear receiver as MF to channel plus precoder reduces the MSE as scaled version of the transmit covariance matrix R_s. The MSE is identical for each data stream;
- in the joint ZF-SNR case, the channel is perfectly inverted and the equal-error constraint results in an identical MSE on each data stream, as in the two other cases.

The joint MF (which is identical to the semi-joint MF) achieves optimum performance at very low SNR. A situation in which interference suppression is less important because of the high noise power compared to the signal power. However, the joint MF saturates at high SNR since it only

transmits one data stream over the strongest eigenmode of the channel.

Fig. 4 shows the uncoded BER as function of the transmit SNR. Comparing the BER among the WF strategies we see that the TX-only WF achieves best performance. This result seems surprising on the first hand, since the transmission strategy with the least computational effort and the most simple receiver structure (only a scalar WF) achieves the best performance. However, this results can be explained by the fact, that the other WF strategies (joint and semi-joint WF) are suffering from the fixed modulation set. Both, the joint WF solution, and the semi-joint WF solution switch off data streams at low and medium SNR. With the assumption of a fixed modulation scheme of QPSK and the fixed transmission rate of 8 bits per channel use, always 4 data streams have to be transmitted. This leads to 50% BER on the neglected data streams, opposite to the TX-only WF where no data streams are neglected. Giving up the assumption of a fixed modulation scheme will improve the performance of the joint and semi-joint transmission strategies as we will see in the next subsection.

The semi-joint ZF and the TX-only ZF approach have identical performance with respect to the uncoded BER due to their identical MSE. Note, that the joint ZF approach outperforms the joint WF approach for high SNR. This effect can also be explained by the constraint of a fixed modulation set that leads to a degradation of the WF approaches that switches off data streams at specific SNR ranges.

The joint MF saturates at 37.5% BER. This saturation level is very clear, since all but one data stream are suppressed in the joint MF approach.

$$\text{BER}_{\text{MF}}(\gamma \to \infty) = \tfrac{1}{4}(3 \cdot 50\% + 0\%) = 37.5\%.$$

6.2. Adaptive modulation

The simplest approach to obtain a data rate of b bits per channel use is to uniformly distribute the b bits onto the D data streams and to use the same, fixed modulation alphabet for each data stream, as performed in the previous subsection. The key assumptions of this strategy are a fixed data rate and a fixed modulation scheme. It has been shown in the previous subsection that this assumptions causes a large restriction to the system performance of the joint and semi-joint transmission approach, since the particular linear precoders have the property of switching off the weakest eigenmodes of the channel.

A more sophisticated approach to achieve the aspired data rate of b bits per channel use is to distribute the b bits onto the D data streams according to an additional optimization criterion which will allocate a higher data rate onto stronger data streams aiming at a minimization of the BER [15,17,9]. This consideration leads to *adaptive modulation*. Since the channel is diagonalized in the joint and semi-joint transmission approach and the strength of each eigenmode is known from the computation of the linear precoding and receive

filter it is possible to compute the SNR of each eigenmode including the amplitude weighting of each data stream for the actual channel realization. With the known SNR it is now possible to numerically compute the *bit-error-probability* for each data stream for a given modulation alphabet a priori as [18]

$$p_i = f(\alpha_i, \text{SNR}_i, \mathcal{M}_i), \quad i = 1, \ldots, D,$$

where p_i, α_i, SNR_i, and $\mathcal{M}_i$ denote the bit-error-probability, the positive real weighting of the symbols, the SNR, and the modulation alphabet of data stream i, respectively. The desired data rate of b bits per channel use is now achieved by distributing the b bits onto the D data streams with appropriate modulation schemes by minimizing the average bit-error probability over all data streams of the actual channel realization:

$$\{\mathcal{M}_{\text{opt},k}\}_{k=1}^D = \underset{\{\mathcal{M}_k\}_{k=1}^D}{\arg\min} \overline{\text{BEP}}$$

$$\text{s.t.} \quad \sum_{i=1}^D \log_2 |\mathcal{M}_i| = b, \tag{16}$$

where the average bit-error-probability reads as

$$\overline{\text{BEP}} = \frac{1}{b} \sum_{i=1}^D f(\alpha_i, \text{SNR}_i, \mathcal{M}_i) \log_2 |\mathcal{M}_i|$$

and $\log_2 |\mathcal{M}_i|$ is the number of bits that are assigned to modulation alphabet $\mathcal{M}_i$. The constraint in (16) ensures a fixed data rate of b bits per channel use.

The distribution of the data onto the eigenmodes of the channel that have been chosen in the optimization process might result in a further reduction of the number of used data streams. Consider the case where the optimization result consists of two data streams where the second stream has a lower SNR compared to the first data stream. If the SNR difference is large enough, it might be advantageous to minimize to the total BER by putting all data onto the stronger eigenmode by choosing an appropriate high order modulation scheme. If the number of used data streams has been reduced by the optimization in Eq. (16) the transmit power P_t consequently has to be re-allocated according to the actual optimization approach. In particular, the number of data streams D is reduced to D' and the power allocation is being recomputed with $D' < D$ to fulfill the transmit power constraint while re-computing the linear precoder F and the linear receiver G. However, the number of used transmit and receive antennas remains unchanged. Note, that in the case of joint TX/RX optimization both sides of the communication link have perfect channel knowledge. Consequently, both sides of the communication link can perform the additional optimization with respect to the modulation scheme in Eq. (16). In the case of the semi-joint optimization the receiver is only a matched filter to the channel plus linear precoder. If we assume that the receiver is notified
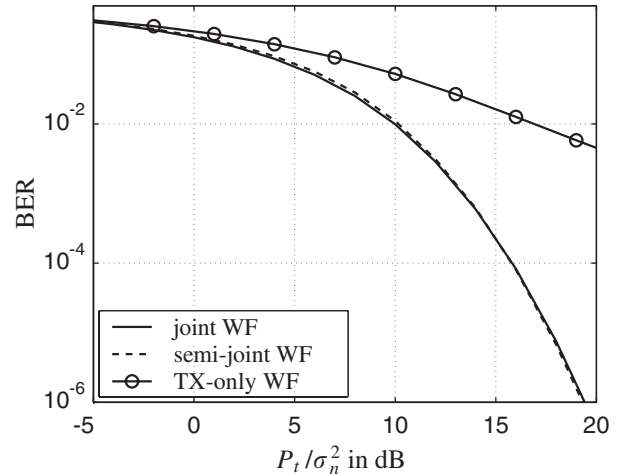

Fig. 5. BER of the three WF transmission strategies as function of the transmit SNR for the use of adaptive modulation.

Table 1. Used modulation set with adaptive modulation

Modulation sets	
256-QAM	8 bits
64-QAM, QPSK	6 + 2 bits
16-QAM, 16-QAM	4 + 4 bits
16-QAM, QPSK, QPSK	4 + 2 + 2 bits
QPSK, QPSK, QPSK, QPSK	2 + 2 + 2 + 2 bits

about the used modulation set,[2] adaptive modulation is also applicable.

A diagonalization of the channel is not achieved with TX-only processing. Adaptive modulation is not applicable with the simplest receiver structure consisting only of a scalar WF, as the remaining interference leads to a prohibitive computational complexity.

Fig. 5 shows the uncoded BER as function of the transmit SNR for the three WF approaches with adaptive modulation. The possible modulation sets are given in Table 1. In comparison to Fig. 4 the BER of the joint and semi-joint WF obtain a large performance increase. Both BER curves even obtain a higher slope for high SNR, which indicates a higher order of exploited diversity. This increase of exploited diversity can be explained by the re-distribution of the data rate onto the number of existing data streams. No data is lost as in the case of a fixed modulation set. Especially at low and medium SNR, where the joint and semi-joint WF optimization switches off data streams, the constant number of $M_R = 4$ receive antennas offer a higher order of diversity compared to the WF approaches with fixed modulation scheme.

---

[2] This requires only very little information. If we have K modulation sets, we require $\lceil \log_2(K) \rceil$ bits to inform the receiver.
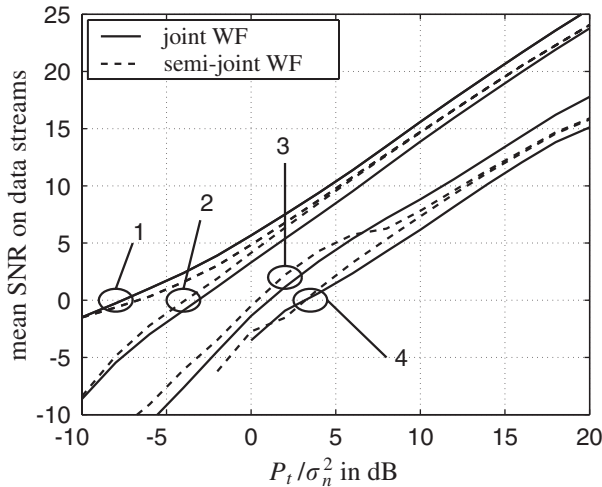
Fig. 6. Mean SNR on the data streams for the joint WF and semi-joint WF, where data stream 1 has highest SNR, data stream 2 has second highest SNR.

Also note, that the semi-joint WF slightly outperforms the joint WF for very high SNR, despite the simpler receiver structure. This higher performance can be explained by a more favorable statistic of the SNR on the individual data streams in the case of the semi-joint WF compared to the joint WF. Fig. 6 shows the mean SNR of the used data streams in the case of the joint WF and the semi-joint WF, where in each case data stream 1 has highest SNR, data stream 2 has second highest SNR, and so on, due to the ordered EVD (see Eq. (2)). In the whole SNR range the strongest eigenmode in the case of the joint WF has always a higher mean SNR compared to the strongest eigenmode of the semi-joint WF. At low and medium SNR range the data is mostly put into the strongest or the two strongest eigenmodes. In this case it is advantageous if the eigenmode containing the biggest portion of the data (which is the strongest eigenmode) has a higher SNR. However, at high SNR ranges the solution of the joint and semi-joint WF with adaptive modulation tend to uniformly distribute the data onto all eigenmodes. In this case the data stream with the lowest mean SNR is limiting the BER performance. Since the fourth eigenmode of the joint WF has a lower mean SNR compared to the fourth eigenmode of the semi-joint WF, the BER performance of the joint WF is suffering from this effect at high SNR.

6.3. Influence of spatial correlations

All previously presented simulation results of Sections 6.1 and 6.2 were performed for frequency-flat uncorrelated Rayleigh fading channel realizations $\boldsymbol{H} \in \mathbb{C}^{M_R \times M_T}$, where the matrix entries $h_{i,j}$ are i.i.d. complex Gaussian distributed with zero mean and unit variance. This type of channel models transmission situations where both the transmitter and the receiver are located in a dense scattering environment.

To get an insight into the effects of spatial correlations at the transmitter and the receiver onto the uncoded BER we modify the generation of the frequency-flat channel $\boldsymbol{H}$ to produce pre-defined correlation matrices at the transmitter side and receiver side, where we take a set of correlation matrices from the 3GPP standardization proposal of [19] to obtain realistic spatial correlations. The used set of correlation matrices at the transmitter and receiver is taken from the standardization scenario #3.

Since a channel scenario with spatial correlations has non-trivial long-term properties, it is also possible to perform signal processing based only on the long-term properties of the channel, i.e. based on the statistics of the channel. This procedure has the advantage of reduced computational complexity and a reduction of required channel knowledge at the transmitter. Note, that long-term properties are slow-changing characteristics of the channel which allows for a more accurate estimation due to a longer time period that is available to perform this estimation [20].

6.3.1. Instantaneous channel knowledge

Figs. 7 and 8 show the uncoded BER as function of the transmit SNR in a correlated channel scenario for fixed modulation and adaptive modulation, respectively.

Fig. 7 shows the uncoded BER of the ZF and WF strategy for the three linear transmission approaches TX-only, joint and semi-joint optimization with fixed modulation. In comparison to Fig. 4, where the channel is uncorrelated, we see that the performance is drastically decreased in each case. This behavior can be explained by the more dispersive eigenmodes of the channel. Since the fixed data rate and the fixed modulation set of QPSK requires the use of all eigenmodes the overall performance is suffering from the degeneration of the weakest eigenmode of the channel. The ZF strategies are suffering most in this situation. As in
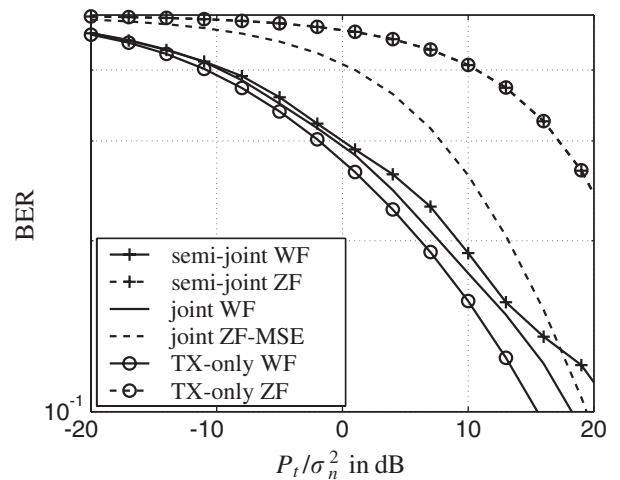

Fig. 7. BER of the three transmission strategies for ZF and WF as function of the transmit SNR for fixed modulation in a correlated channel scenario.
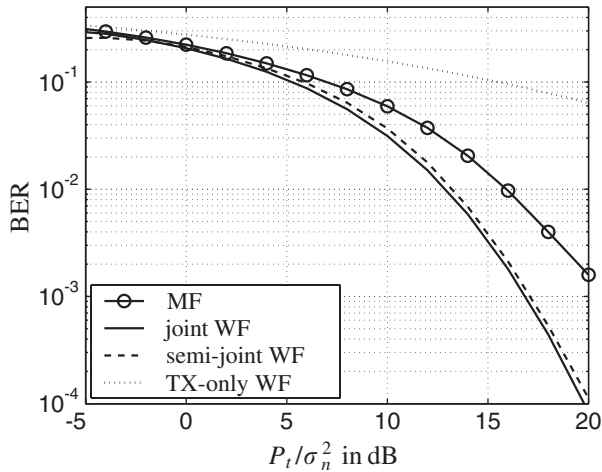
Fig. 8. BER of the MF, and WF transmission strategies as function of the transmit SNR for the use of adaptive modulation in a correlated channel scenario.
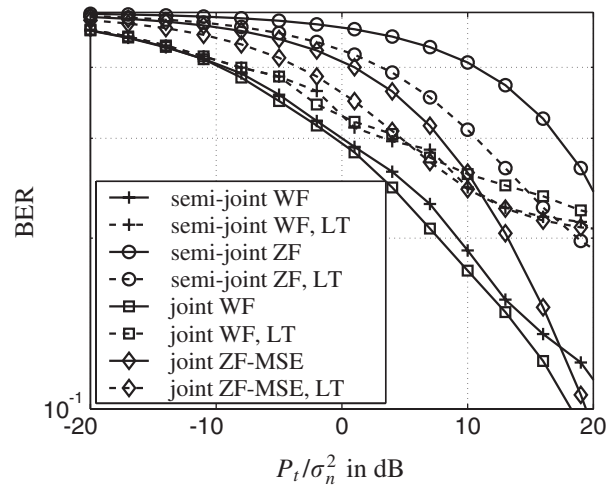

Fig. 9. BER of joint and semi-joint ZF and WF as function of the transmit SNR for fixed QPSK modulation in a correlated channel scenario. The solid lines are instantaneous channel knowledge, while the dashed lines are long-term channel knowledge at the transmitter.

the case of the uncorrelated channel situation the TX-only WF again achieves best performance. Note the ripples in the BER curve of the joint and semi-joint WF curves at an SNR level of 12 dB. Due to the given spatial correlation matrices in this correlated channel scenario the waterfilling behavior of the joint and semi-joint WF approaches to switch off the weakest eigenmodes is much more associated with a certain SNR level, compared to the uncorrelated channel scenario where the waterfilling behavior is more smooth over the abscissa (SNR).

Fig. 8 shows the MF and WF strategies of the joint and semi-joint optimization with adaptive modulation in the same correlated channel situation as in Fig. 7. We see that the adaptive modulation can compensate a lot for the more dispersive eigenvalues of the channel. However, in comparison to Fig. 5 with the uncorrelated channel situation each transmission concept is still losing in performance. Note, that the degradation of the joint and semi-joint MF approach has decreased due to the increase of the strongest eigenvalue in the correlated channel situation. In comparison to Fig. 7 the ripples of the WF approaches have vanished. The BER curve of the TX-only WF with fixed QPSK modulation in this correlated channel situation is given as dotted line for reference.

6.3.2. Long-term channel knowledge

The derived transmission approaches of joint TX/RX optimization and semi-joint optimization can also be performed on a long-term basis by taking the eigenbase V_{LT} and the eigenvalues Λ_{LT} not of the instantaneous channel covariance R_H, but rather performing an EVD of the long-term average

$$E\{R_H\} = V_{LT} \Lambda_{LT} V_{LT}^H.$$

With this simplification of the channel knowledge, the linear precoders of the joint TX/RX optimization and semi-

joint optimization are now computed based on the long-term eigenbase V_{LT} and eigenvalues Λ_{LT}.

The linear receivers have knowledge about the instantaneous channel realization H but the EVD is only performed on a long-term basis to compute the long-term eigenbase V_{LT} and eigenvalues Λ_{LT} (see Eq. (2)). No EVD of the channel is performed at the receiver. As consequence, the MIMO channel is no longer diagonalized in each channel realization H. The diagonalization only takes place on average.

Fig. 9 shows the uncoded BER as function of the transmit SNR for the joint and semi-joint ZF and WF approach, where the solid lines represent the usage of the instantaneous eigenbase and eigenvalues, while the dashed lines represent the usage of the long-term eigenbase and eigenvalues. The consequence of LT processing is that the MIMO channel is no longer diagonalized in each channel realization H. Therefore the LT approaches are now experiencing inter-stream-interference. This interference leads to a saturation of the BER curves at high SNR.

Note, that the BERs of the LT WF approaches are worse compared to the corresponding WF approaches utilizing the instantaneous eigensystem. However, the LT ZF approaches outperform the corresponding ZF approaches utilizing the instantaneous eigensystem at low SNR. This can be explained by the zero-forcing condition of the ZF approaches, where the inversion of the channel in the case of instantaneous knowledge might also contain channel situations with large eigenvalue spread which lead to a rather high SNR degradation. In the case of LT knowledge the inversion of the channel is only performed on average, where the SNR degradation is not so high as in the case of instantaneous knowledge, however at the price of inter-stream-interference which leads to a saturation of the BER curves. Obviously it is more advantageous to have higher interference and lower
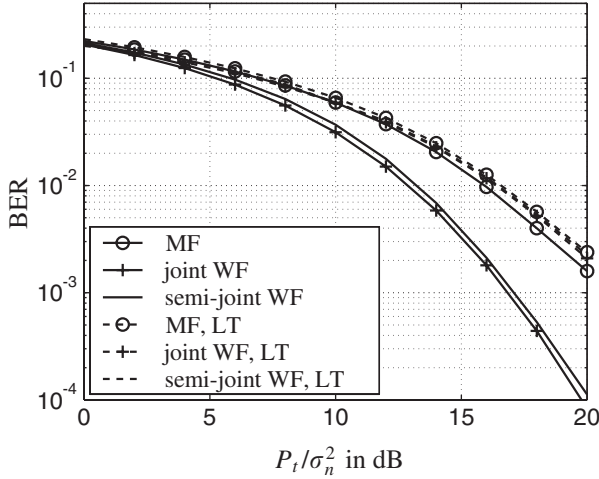
Fig. 10. BER of the MF, and WF transmission strategies as function of the transmit SNR with adaptive modulation in a correlated channel scenario. The solid lines are instantaneous channel knowledge, while the dashed lines are long-term channel knowledge at the transmitter.

SNR degradation, compared to no interference and higher SNR degradation in the case of the ZF approaches at low and medium SNR.

Fig. 10 shows the uncoded BER as function of the transmit SNR for the joint and semi-joint MF and WF approaches with adaptive modulation in a correlated channel scenario. The usage of instantaneous knowledge is given as solid lines, while the usage of long-term channel knowledge is given as dashed lines. For clearness the curves of the ZF approaches are not shown.

The performance of the joint/semi-joint MF is only degrading by a rather tiny amount when assuming only long-term knowledge of the eigenbase. Obviously the dominant eigenmode varies only by a small amount between different channel realization H.

The BER performance of the joint and semi-joint WF degrade strongly and achieve the same performance as the LT MF when assuming knowledge not of the instantaneous eigenbase but of the long-term eigenbase. Since the eigenbase and the eigenvalues are only known on a long-term basis, adaptive modulation also can be performed only on long-term basis. The choice of the modulation set merely depends on the SNR level, and the long-term statistics of the channel, which is constant. Because of the correlations of the channel model, the first eigenmode is very dominant. Obviously the dominant eigenmode is large enough that the adaptive modulation allocates only one data stream on this eigenmode with 256-QAM modulation in the shown SNR range.

7. Conclusion

In this article we have proposed a new linear transmission strategy with a simple MF receiver structure and a

precoder optimization according to the matched filter, zero-forcing, and minimum mean-square error principle. This new transmission concept accomplishes a diagonalization of the MIMO channel into its eigenmodes, similar to a joint TX/RX optimization, however, at a much lower computational cost for the receiver side. It has further been shown that with respect to the BER the proposed system concept has comparable performance as the joint TX/RX optimization scheme in the case of adaptive modulation. At high SNR the new transmission concept even outperforms joint TX/RX optimization due to a more favorable statistic of the scalar weightings of the diagonalized MIMO channel, compared to the joint TX/RX case.

Appendix A.

A.1. Computation of the semi-joint MF

Note that the SNR γ and the transmit power constraint for the optimization of the semi-joint MF in Eq. (10) are independent of the scalar receive weighting g. Therefore, we have that $g \in \mathbb{R}$ is arbitrary.

The Lagrangian function for the semi-joint MF optimization approach is given as (cf. Eq. (9))

$$L(F, g, \mu) = \frac{\sigma_s^2 \, \text{tr}(F^H R_H F)}{D} - \mu[\sigma_s^2 \, \text{tr}(FF^H) - P_t].$$

Differentiating the Lagrangian function with respect to F^* provides the KKT condition

$$\frac{\partial L}{\partial F^*} = 0 : 0 = \frac{\sigma_s^2}{D} R_H F - \sigma_s^2 \mu F. \tag{A.1}$$

By taking the vec($\cdot$) operator of the above KKT condition and applying the properties of the vec($\cdot$) operator[3] we can re-write the above equation as

$$\frac{1}{D}[\mathbf{1} \otimes R_H]\text{vec}(F) = \mu \, \text{vec}(F). \tag{A.2}$$

Eq. (A.2) is an eigenvalue problem. Performing the sorted *eigenvalue decomposition* (EVD) of R_H from Eq. (2) and using a property of the Kronecker product[4] we can conclude, that

$$\text{vec}(F) = \beta c \otimes v_i,$$

where v_i is the ith column of the eigenvectors V and β is a scalar weighting. Note, that any arbitrary $c \in \mathbb{C}^D$ is an eigenvector of the identity matrix $\mathbf{1}$ belonging to the eigenvalue 1. In other words

$$F = \beta v_i c^T.$$

---

[3] $\text{vec}(ABC) = (C^T \otimes A)\text{vec}(B)$ as given in [21].

[4] If a is an eigenvector of A with eigenvalue α and b is an eigenvector of B with eigenvalue β then $a \otimes b$ is an eigenvector of $A \otimes B$ with eigenvalue $(\alpha \cdot \beta)$, see [21].

The Lagrangian multiplier μ is the corresponding eigenvalue λ_i divided by D. If we left-multiply Eq. (A.1) with $\boldsymbol{F}^{\mathrm{H}}$ and take the trace of the result we obtain utilizing the transmit power constraint in Eq. (10)

$$\gamma = \frac{\mathrm{tr}(\boldsymbol{F}^{\mathrm{H}}\boldsymbol{R}_H\boldsymbol{F})\sigma_s^2}{D} = \mu P_t,$$

where γ is the cost function we want to maximize in Eq. (10). Consequently, we have to choose the eigenvector $\boldsymbol{v}_1$ of $\boldsymbol{R}_H$ that belongs to the maximum eigenvalue λ_1. With the transmit power constraint we obtain as solution

$$\boldsymbol{F}_{\mathrm{MF}}^{\mathrm{semi}} = \sqrt{\frac{P_t}{\sigma_s^2}}\boldsymbol{v}_1\frac{\boldsymbol{c}^{\mathrm{T}}}{\|\boldsymbol{c}\|_2}. \qquad (A.3)$$

Remember that $g \in \mathbb{R}$ is arbitrary. To correctly recover the signal amplitude of the transmitted data sequence $\boldsymbol{s}[k]$ we apply a scalar WF after the filter output which computes as

$$g_{\mathrm{MF}}^{\mathrm{semi}} = \frac{1}{P_t\lambda_1 + 1} \in \mathbb{R}_+. \qquad (A.4)$$

A.2. Computation of the semi-joint ZF

The Lagrangian function for the optimization of the semi-joint ZF in Eq. (12) is

$$\begin{aligned} L(\boldsymbol{F}, g, \mu, \boldsymbol{\Omega}) = {} & gD - \mu[\sigma_s^2\,\mathrm{tr}(\boldsymbol{F}\boldsymbol{F}^{\mathrm{H}}) - P_t] \\ & - 2\,\mathrm{Re}\{\mathrm{tr}[\boldsymbol{\Omega}(g\boldsymbol{F}^{\mathrm{H}}\boldsymbol{R}_H\boldsymbol{F} - \boldsymbol{1})]\}, \end{aligned} \qquad (A.5)$$

where $\mu \in \mathbb{R}$ and $\boldsymbol{\Omega} \in \mathbb{C}^{D\times D}$ are Lagrangian multipliers. Differentiating the Lagrangian function with respect to $\boldsymbol{F}^*$ and g gives the KKT conditions

$$\frac{\partial L}{\partial \boldsymbol{F}^*} = \boldsymbol{0} : \boldsymbol{0} = -g\boldsymbol{R}_H\boldsymbol{F}\boldsymbol{\Omega} - g\boldsymbol{R}_H\boldsymbol{F}\boldsymbol{\Omega}^{\mathrm{H}} - \sigma_s^2\mu\boldsymbol{F},$$

$$\frac{\partial L}{\partial g} = 0 : 0 = D - 2\,\mathrm{tr}(\boldsymbol{\Omega}\boldsymbol{F}^{\mathrm{H}}\boldsymbol{R}_H\boldsymbol{F} + \boldsymbol{F}^{\mathrm{H}}\boldsymbol{R}_H\boldsymbol{F}\boldsymbol{\Omega}^{\mathrm{H}}).$$

From the second KKT condition we can make the substitution $\boldsymbol{M} = \boldsymbol{\Omega} + \boldsymbol{\Omega}^{\mathrm{H}}$ which simplifies the KKT conditions to

$$g\boldsymbol{R}_H\boldsymbol{F}\boldsymbol{M} + \sigma_s^2\mu\boldsymbol{F} = \boldsymbol{0},$$

$$D - 2\,\mathrm{tr}(\boldsymbol{F}^{\mathrm{H}}\boldsymbol{R}_H\boldsymbol{F}\boldsymbol{M}) = 0.$$

Left-multiplying the first equation with $\boldsymbol{F}^{\mathrm{H}}$ and utilizing the zero-forcing constraint $g\boldsymbol{F}^{\mathrm{H}}\boldsymbol{R}_H\boldsymbol{F} = \boldsymbol{1}$ we directly obtain the solution

$$\boldsymbol{M} = -\sigma_s^2\mu\boldsymbol{F}^{\mathrm{H}}\boldsymbol{F}.$$

Re-inserting this in the first KKT condition leads to the equation

$$\boldsymbol{F} = g\boldsymbol{R}_H\boldsymbol{F}\boldsymbol{F}^{\mathrm{H}}\boldsymbol{F}. \qquad (A.6)$$

By performing the eigenvalue decomposition $\boldsymbol{R}_H$ according to Eq. (2) and a singular-value decomposition of $\boldsymbol{F}$ as follows

$$\boldsymbol{F} = \boldsymbol{U}_F\boldsymbol{\Sigma}_F\boldsymbol{V}_F^{\mathrm{H}} \in \mathbb{C}^{M_{\mathrm{T}}\times D} \qquad (A.7)$$

with $\boldsymbol{\Sigma}_F \in \mathbb{R}_{0,+}^{D\times D}$, Eq. (A.6) modifies after some simplifications to

$$\boldsymbol{\Sigma}_F^{-2} = g\boldsymbol{U}_F^{\mathrm{H}}\boldsymbol{R}_H\boldsymbol{U}_F.$$

The right-hand side has to be diagonal. Consequently, we can conclude, that the left-hand side singular vectors $\boldsymbol{U}_F$ of $\boldsymbol{F}$ are identical with the eigenvectors $\boldsymbol{V}$ of $\boldsymbol{R}_H$, except for a permutation $\boldsymbol{\Pi}$:

$$\boldsymbol{U}_F = \boldsymbol{V}\boldsymbol{\Pi} \quad \text{with} \quad \boldsymbol{\Pi} \in \{0, 1\}^{D\times D}. \qquad (A.8)$$

Eq. (A.6) now simplifies to

$$\boldsymbol{\Sigma}_F^{-2} = g\boldsymbol{\Pi}^{\mathrm{T}}\boldsymbol{\Lambda}\boldsymbol{\Pi}.$$

The linear transmit processing can now be written as

$$\boldsymbol{F} = \frac{1}{\sqrt{g}}\boldsymbol{V}\boldsymbol{\Lambda}^{-1/2}\boldsymbol{\Pi}\boldsymbol{V}_F^{\mathrm{H}}.$$

Inserting this in the transmit power constraint gives[5]

$$\begin{aligned} P_t &= \sigma_s^2\,\mathrm{tr}(\boldsymbol{F}\boldsymbol{F}^{\mathrm{H}}) \\ &= \frac{\sigma_s^2}{g}\,\mathrm{tr}(\boldsymbol{V}\boldsymbol{\Lambda}^{-1/2}\boldsymbol{\Pi}\boldsymbol{V}_F^{\mathrm{H}}\boldsymbol{V}_F\boldsymbol{\Pi}^{\mathrm{T}}\boldsymbol{\Lambda}^{-1/2}\boldsymbol{V}^{\mathrm{H}}) \\ &= \frac{\sigma_s^2}{g}\,\mathrm{tr}(\boldsymbol{\Lambda}^{-1}), \end{aligned}$$

where we can conclude

$$g_{\mathrm{ZF}}^{\mathrm{semi}} = \frac{\sigma_s^2\,\mathrm{tr}(\boldsymbol{\Lambda}^{-1})}{P_t}. \qquad (A.9)$$

Note, that $g_{\mathrm{ZF}}^{\mathrm{semi}}$ is the cost function we want to optimize (cf. Eq. (A.5)). Since the cost function is neither a function of the permutation $\boldsymbol{\Pi}$ nor of the right-hand side singular vectors $\boldsymbol{V}_F$ we choose both as identity matrices. The solution for the semi-joint ZF evolves as

$$\boldsymbol{F}_{\mathrm{ZF}}^{\mathrm{semi}} = \sqrt{\frac{P_t}{\sigma_s^2\,\mathrm{tr}(\boldsymbol{\Lambda}^{-1})}}\boldsymbol{V}\boldsymbol{\Lambda}^{-1/2}. \qquad (A.10)$$

A.3. Computation of the semi-joint WF

The Lagrangian function for the optimization of the semi-joint WF in Eq. (14) is given as

$$\begin{aligned} L(\boldsymbol{F}, g, \mu) = {} & \mathrm{tr}\left[(g\boldsymbol{F}^{\mathrm{H}}\boldsymbol{R}_H\boldsymbol{F} - \boldsymbol{1})^2\sigma_s^2 + g^2\boldsymbol{F}^{\mathrm{H}}\boldsymbol{R}_H\boldsymbol{F}\right] \\ & - \mu[\sigma_s^2\,\mathrm{tr}(\boldsymbol{F}\boldsymbol{F}^{\mathrm{H}}) - P_t], \end{aligned}$$

where $\mu \in \mathbb{R}$ is the Lagrangian multiplier for the transmit power constraint. The KKT conditions are

$$\boldsymbol{0} = 2g^2\sigma_s^2\boldsymbol{R}_H\boldsymbol{F}\boldsymbol{F}^{\mathrm{H}}\boldsymbol{R}_H\boldsymbol{F} + (g^2 - 2g\sigma_s^2)\boldsymbol{R}_H\boldsymbol{F} - \mu\sigma_s^2\boldsymbol{F},$$

$$0 = 2g\sigma_s^2\,\mathrm{tr}((\boldsymbol{F}^{\mathrm{H}}\boldsymbol{R}_H\boldsymbol{F})^2) + (2g - 2\sigma_s^2)\mathrm{tr}(\boldsymbol{F}^{\mathrm{H}}\boldsymbol{R}_H\boldsymbol{F}).$$

---

[5] Note the property of the permutation matrix $\boldsymbol{\Pi}\boldsymbol{\Pi}^{\mathrm{T}} = \boldsymbol{\Pi}^{\mathrm{T}}\boldsymbol{\Pi} = \boldsymbol{1}$.

To obtain the solution we perform an eigenvalue decomposition of R_H according to Eq. (2) and perform an SVD of F as in Eq. (A.7). The first KKT condition reads after some simplifications as

$$2g^2\sigma_s^2 U_F^H R_H U_F \Sigma_F^2 U_F^H R_H U_F \Sigma_F^2$$
$$+ (g^2 - 2g\sigma_s^2) U_F^H R_H U_F \Sigma_F^2 = \mu\sigma_s^2 \Sigma_F^2.$$

We can conclude that the left-hand side singular vectors U_F have to be identical to the eigenbase V up to a permutation $\Pi \in \{0,1\}^{D\times D}$:

$$U_F = V\Pi,$$

since the right-hand side of above equation is diagonal. For notational convenience we substitute $\hat{\Lambda} = \Pi^T \Lambda \Pi$. With these assumptions the KKT conditions evolve now as

$$0 = 2g\sigma_s^2(g\Sigma_F^2\hat{\Lambda} - 1)\hat{\Lambda}\Sigma_F + g^2\hat{\Lambda}\Sigma_F - \mu\sigma_s^2\Sigma_F,$$

$$0 = 2g\sigma_s^2 \operatorname{tr}(\Sigma_F^4\hat{\Lambda}^2) - 2\sigma_s^2 \operatorname{tr}(\Sigma_F^2\hat{\Lambda}) + 2g \operatorname{tr}(\Sigma_F^2\hat{\Lambda}).$$

From the second KKT condition we can solve for g as

$$g = \frac{\sigma_s^2 \operatorname{tr}(\Sigma_F^2\hat{\Lambda})}{\operatorname{tr}\left(\sigma_s^2\Sigma_F^4\hat{\Lambda}^2 + \Sigma_F^2\hat{\Lambda}\right)}. \qquad (A.11)$$

Re-arranging the first KKT condition leads to

$$2g\sigma_s^2\Sigma_F^3\hat{\Lambda}^2 + (g - 2\sigma_s^2)\hat{\Lambda}\Sigma_F - \mu'\sigma_s^2\Sigma_F = 0,$$

where we have scaled the Lagrangian multiplier as $\mu' = \mu/g$. We obtain with the substitution

$$\varepsilon = \frac{2g\sigma_s^2}{2\sigma_s^2 - g} \qquad (A.12)$$

after another scaling of the Lagrangian multiplier that Σ_F follows from

$$\left[\varepsilon\Sigma_F^2\hat{\Lambda} - (1 + \mu''\hat{\Lambda}^{-1})\right]\varepsilon\hat{\Lambda}\Sigma_F^2 = 0.$$

By defining the auxiliary variable

$$B = \varepsilon\hat{\Lambda}\Sigma_F^2 \qquad (A.13)$$

we obtain the well-known problem [22]

$$[B - (1 + \mu''\hat{\Lambda}^{-1})]B = 0$$

which has the solution

$$B = (1 + \mu''\hat{\Lambda}^{-1})_+ = \Pi^T\Psi\Pi \qquad (A.14)$$

with $\Psi = (1 + \mu''\Lambda^{-1})_+$. The solution for the semi-joint optimization can be found in an iterative procedure, where the parameter μ'' is chosen such to fulfill the transmit power constraint. Note, that B is always diagonal, positive semi-definite. The original argument of the optimization after back-substituting $\hat{\Lambda} = \Pi^T\Lambda\Pi$ computes as

$$\Sigma_F^2 = \frac{1}{\varepsilon}\hat{\Lambda}^{-1}B$$
$$= \frac{\operatorname{tr}(\Psi)}{2\sigma_s^2 \operatorname{tr}(\Psi - \Psi^2)}\Pi^T\Lambda^{-1}\Psi\Pi. \qquad (A.15)$$

For the linear precoder we get

$$F = U_F\Sigma_F V_F^H$$
$$= \sqrt{\frac{\operatorname{tr}(\Psi)}{2\sigma_s^2 \operatorname{tr}(\Psi - \Psi^2)}}V\Pi\Pi^T\Lambda^{-1/2}\Psi^{1/2}\Pi V_F^H$$
$$= \sqrt{\frac{\operatorname{tr}(\Psi)}{2\sigma_s^2 \operatorname{tr}(\Psi - \Psi^2)}}V\Lambda^{-1/2}\Psi^{1/2}\Pi V_F^H.$$

Inserting this solution of F in the optimization criterion, cf. Eq. (14), shows that neither the cost function nor the transmit power constraint depend on the permutation Π and right-hand side singular vector V_F. Therefore we choose them to be the identity matrix and the solution computes as

$$F_{\text{WF}}^{\text{semi}} = \sqrt{\frac{\operatorname{tr}(\Psi)}{2\sigma_s^2 \operatorname{tr}(\Psi - \Psi^2)}}V\Lambda^{-1/2}\Psi^{1/2} \qquad (A.16)$$

with $\Psi = (1 + \mu''\Lambda^{-1})_+$. The optimum weighting $g_{\text{WF}}^{\text{semi}}$ can be computed by inserting the solution of Eq. (A.15) in Eq. (A.11) which yields

$$g_{\text{WF}}^{\text{semi}} = 2\sigma_s^2 \frac{\operatorname{tr}(\Psi - \Psi^2)}{\operatorname{tr}(2\Psi - \Psi^2)}. \qquad (A.17)$$

References

[1] Verdu S. Multiuser detection. Cambridge, UK: Cambridge University Press; 1998.

[2] Vojčić B, Jang W. Transmitter precoding in synchronous multiuser communications. IEEE Trans Commun 1998;46:1346–55.

[3] Joham M, Utschick W, Nossek J, Linear transmit processing in MIMO communications systems. IEEE Trans Signal Process, 2004, accepted for publication.

[4] Pilc R. The optimum linear modulator for a Gaussian source used with a Gaussian channel. Bell System Tech J 1969;48:3075–89.

[5] Lee K, Petersen D. Optimal linear coding for vector channels. IEEE Trans Commun 1976;COM-24:1283–90.

[6] Salz J. Digital transmission over cross-coupled linear channels. AT&T Tech J 1985;64:1147–59.

[7] Yang J, Roy S. On joint transmitter and receiver optimization for multiple-input-multiple-output (MIMO) transmission systems. IEEE Trans Commun 1994;42:3221–31.

[8] Scaglione A, Giannakis G, Barbarossa S. Redundant filterbank precoders and equalizers, Part I: unification and optimal designs. IEEE Trans Signal Process 1999;47: 1988–2006.

[9] Ban K, Katayama M, Yamazato T, Ogawa A. Joint optimization of transmitter/receiver with multiple transmit/receive antennas in band-limited channels. IEICE Trans Commun 2000;E83-B:1697–704.

[10] Sampath H, Stoica P, Paulraj A. Generalized linear precoder and decoder design for MIMO channels using the weighted MMSE criterion. IEEE Trans Commun 2001;49(12).

[11] Kurpjuhn T. Transmission strategies in wireless MIMO communication systems. Dissertation. Munich, Germany: Munich University of Technology, Institute for Circuit Theory and Signal Processing, April 2004.

[12] Wang J, Zhao M, Zhou S, Yao Y. A novel multipath transmission diversity scheme in TDD-CDMA systems. IEICE Trans Commun 1999;E82-B:1706–9.

[13] Irmer R, Noll Barreto A, Fettweis G. Transmitter precoding for spread-spectrum signals in frequency-selective fading channels. Proc. 3G Wireless, May 2001. p. 939–44.

[14] Han J-K, Lee M-W, Park H-K. Principal ratio combining for pre/post-rake diversity. IEEE Commun Lett 2002;6: 234–6.

[15] Kurpjuhn T, Joham M, Nossek J. Optimization criteria for linear precoding in flat fading TDD–MIMO downlink channels with matched filter receivers. In: Proceedings of the 59th IEEE vehicular technology conference. (Spring VTC '04), Milan, Italy, May 2004.

[16] Scaglione A, Stoica P, Barbarossa S, Giannakis G, Sampath H. Optimal design for space-time linear precoders and decoders. IEEE Trans Signal Process 2002;50:1051–64.

[17] Kiessling M, Speidel J, Viering I, Reinhardt M. Short-term and long-term diagonalization of correlated mimo-channels with adaptive modulation. Proceedings of the 13th IEEE international symposium on personal, indoor and mobile radio communication (PIMRC), Lisboa, Portugal, September 2002, p. 593–7.

[18] Proakis J. Digital communications. 3rd ed., New York, NY: McGraw-Hill; 1995.

[19] Lucent, Nokia, Siemens TI. A standardized set of MIMO radio propagation channels, 2001. 3GPP TSG RAN WG1 #21-1179.

[20] Brunner, C. Utschick, W. Nossek, J. Exploiting the short-term and long-term channel properties in space and time: eigenbeamforming concepts for the BS in WCDMA. Eur Trans Telecommun, 2001; 365–78.

[21] Brewer J. Kronecker products and matrix calculus in system theory. IEEE Trans Circuits Systems 1978;CAS-25:772–81.

[22] Telatar E. Capacity of multi-antenna gaussian channels. Technical Memorandum, Bell Laboratories, Lucent Technologies. Eur Trans Telecommun 1999;10(6):585–95.

the design of filters for communication systems. In 1978, he became supervisor of a group working on discrete-time circuits (switched-capacitor and CCD-filters) and from 1980 on he was as Head of Department responsible for electromechanical, microwave and digital filter design activities. In 1982 he moved into Digital Microwave Radio Design, where he first was responsible for high data rate modems employing multi level modulation techniques. In 1987 he was promoted to Head of all Radio Systems Design. Since 1989 he is a Full Professor for Circuit Theory and Signal Processing at Munich University of Technology, where he teaches undergraduate and graduate courses on circuit and systems theory and signal processing and leads research on signal processing algorithms for communications systems, theory of linear systems and VLSI architectures.

From 1999 till 2002 he was Dean of the Department of Electrical Engineering and Information Technology of the Munich University of Technology.

He has been a guest professor in 1984 at the University of Cape Town, South Africa and in 1992 and 1998 at the University of California at Berkeley and in 1995 at the University of Technology in Vienna.

Prof. Nossek served as Guest Editor for the IEEE Transactions on Circuits and Systems in 1993, as Associate Editor during 1991 to 1993 and as Editor-in Chief during 1995 to 1997. He is on the Editorial Board of a number of scientific and technical journals. He was program co-chairman of the IEEE International Conference on Acoustics, Speech and Signal Processing in Munich in 1997. He was a member of the Board of Governors of the IEEE Circuits and Systems Society from 1998 to 2000. He is a Fellow of IEEE since 1993. His awards include the ITG Best Paper Award 1988, the Mannesmann Mobilfunk Innovations award 1998 and the Golden Jubilee Medal of the IEEE Circuits and Systems Society for "Outstanding Contributions to the Society". He was President Elect of the IEEE Circuits and Systems Society in 2001, President in 2002 and Past President in 2003. Since 2005 he is Vice President of VDE.

Tobias Peter Kurpjuhn was born in 1974 in Ruit auf den Fildern, near Stuttgart, Germany. He received the Dipl.-Ing. and Dr.-Ing. degrees in Electrical Engineering from the Munich University of Technology, Munich, Germany, in 1999 and 2004, respectively.

In the summer of 1998 he stayed at the University of Illinois at Urbana-Champaign where he worked on the development of a man-machine-interface for robotic arms within the scope of an internship in the Artificial Intelligence Lab at the Beckman Institute. From 1999 to 2004 he was a Research Assistant in the Institute for Circuit Theory and Signal Processing at the Munich University of Technology. Since 2004, he works in the Concept Engineering Department at Infineon Technologies, Munich, focusing on the development of baseband algorithms for GSM and EDGE. He also works on the development and application of signal processing algorithms to current and future MIMO systems.

Josef A. Nossek was born on December 17, 1947 in Vienna, Austria. He received the Dipl.- Ing. and the Dr. techn. degrees in Electrical Engineering from the University of Technology in Vienna, Austria in 1974 and 1980, respectively.

In 1974, he joined Siemens AG in Munich, Germany, as a member of the Technical Staff, where he worked on

Michael Joham was born in 1974 in Kufstein, Austria. He received the Dipl.-Ing. and Dr.-Ing. degrees (both with summa cum laude) in electrical engineering from the Munich University of Technology (TUM) in 1999 and 2004, respectively.

He has been with the Institute of Circuit Theory and Signal Processing at the TUM. Since 1999, where he is currently a senior researcher. In the summers of 1998 and 2000, he visited the Purdue University,

His main research interests are estimation theory, reduced-rank processing, and precoding in mobile communications.

Dr. Joham received the VDE Preis for his diploma thesis in 1999 and the Texas-Instruments-Preis for his dissertation in 2004.